Research Square

Preprints are preliminary reports that have not undergone peer review.
They should not be considered conclusive, used to inform clinical practice,
or referenced by the media as validated information.

Comparative study of the secondary metabolites of three Curcuma species and their anticancer activity in Hela and SAS cells

Khetbadei Lysinia Hynniewta Hadem

khet21@gmail.com

Indian Council of Agricultural Research NEH Region, Umiam, Meghalaya, India

Arnab Sen

Indian Council of Agricultural Research NEH Region, Umiam, Meghalaya, India

Kekungu-u Puro

Indian Council of Agricultural Research NEH Region, Umiam, Meghalaya, India

Article

Keywords: Apoptosis, Curcuma angustifolia (CAu), Curcuma amada (CAm), Curcuma caesia (CCa), Caspases, p53, secondary metabolites

Posted Date: November 24th, 2026

DOI: https://doi.org/10.21203/rs.3.rs-11529595/v1

License: This work is licensed under a Creative Commons Attribution 4.0 International License.
Read Full License

Additional Declarations: No competing interests reported.

Title of the study: Comparative study of the secondary metabolites of three Curcuma species and their anticancer activity in Hela and SAS cells.

Authors:

1) Dr. Khetbadei Lysinia Hynniewta Hadem [1,2,a]
   Senior Demonstrator,
   Email: khet21@gmail.com
   ORCID ID: 0000-0002-4278-3942
   Phone no: +91 9862616968

2) Dr. Arnab Sen [1,3,b]
   Principal Scientist & Head
   Email: arnabsen123@gmail.com
   Phone no: +91 8974027632

3) Dr. Kekungu-u Puro [1]
   Principal Scientist
   Email: akulepuro@rediffmail.com
   Phone no: +91 8787338901

[1] Division of Animal Health,
Indian Council of Agricultural Research NEH Region,
Umiam, Meghalaya, India

[2] Department of Biochemistry,
All India Institute of Medical Sciences
New Delhi - 110029, India.

[3] ICAR-Indian Veterinary Research Institute,
Eastern Regional Station (ERS),
Kolkata, India.

[a] Dr. Khetbadei Lysinia Hynniewta Hadem was affiliated to '1' at the start and '2' at the time of submission for publication.

[b] Dr. Arnab Sen was affiliated to '1' at the start and '3' at the time of submission for publication.

Corresponding Author:

Dr. Khetbadei Lysinia Hynniewta Hadem

Senior Demonstrator, Department of Biochemistry,

All India Institute of Medical Sciences

New Delhi - 110029, India.

Email: khet21@gmail.com

ORCID ID: 0000-0002-4278-3942

Phone no: +91 9862616968

Abstract: Traditional medicines are still largely used by many communities in the world to treat various ailments and they are lately integrated into conventional therapy for the overall health and wellness of the patient. A scientific understanding of the effectiveness of these herbal plants is highly required so they can be used as complementary medicine or as potential drug sources. This study therefore aims to evaluate the effectiveness of *Curcuma angustifolia* (CAu), *Curcuma amada* (CAm) and *Curcuma caesia* (CCa) in cancer treatment through the induction of apoptotic pathway in HeLa and SAS cancer cell lines. The induction of apoptosis of these cells were monitored by evaluating caspases 3, 8 and 9, Cdk1 and p53 expression. Post treatment with CAu, CAm and CCa for 24 h caused a downregulation of Cdk1 in both cells. p53 in SAS cells was upregulated post treatment with all the curcuma species whereas in HeLa cells p53 was upregulated only by CAm and CCa. Caspases 8, 9 and 3 was also activated

leading to apoptosis of cells. Different metabolites present in the three curcuma species played a role in inducing apoptosis of HeLa and SAS cells. The three curcuma species are rich sources of potential anticancer drugs/complementary medicine.

Keywords: Apoptosis, *Curcuma angustifolia* (CAu), *Curcuma amada* (CAm), *Curcuma caesia* (CCa), Caspases, p53, secondary metabolites.

INTRODUCTION

The global cancer burden is continually increasing accounting for 9.7 million deaths and 20.6 million new cancer cases in 2024. Lip, oral cavity and cervix uteri are in the top 5 most frequent cancer in India according to the GLOBOCAN 2024 estimates of cancer incidence and mortality as per the data of the International Agency for Research on Cancer [1]. North East region of India recorded the highest cancer incidence with low survival rate than other areas in the country; this is mainly due to lack of specialized treatment facilities [2].

Traditional medicine (TM) has contributed to the global health status and many countries have adopted the integration of traditional and complementary medicine along with conventional therapy for the treatment and management of cancer [3-6]. The *WHO Traditional Medicine Strategy 2014-2023* goals is "harnessing the potential contribution of TM to health, wellness and people centred health care; and promoting the safe and effective use of TM by regulating, researching and integrating TM products, practitioners and practice into health systems, where appropriate" [7]. One of the challenges in implementing this strategy is insufficient scientific evidence of the efficacy and safety of TM. The contribution of this study is to the scientific understanding of the medicinal properties and effectiveness of three curcuma species, *Curcuma angustifolia* (CAu), *Curcuma amada* (CAm) and *Curcuma caesia* (CCa) as potential drugs/source of drugs in cancer treatment. The three curcuma species belong to the Zingiberaceae family and they grow wildly in Meghalaya, North east, India [8,9]. These species are used extensively in traditional medicine and some studies have reported their biological properties and in particular their anticancer activity [10-17]. It is well known that plants secondary metabolites play a role in their biological and medicinal properties. Comparison of these metabolites in the ethyl acetate fraction of the three plant species was carried out by liquid chromatography coupled to high resolution mass spectrometry (LC-HRMS) in order to give us an insight as to what metabolites are responsible for their biological activity and whether the three plant species contain a similar metabolite profile. The anticancer effect of the

ethyl acetate fraction of each curcuma species if any were carried out in two cell lines; HeLa which is a cervix carcinoma and SAS which is an oral squamous cell carcinoma. One of the mechanism by which cancer cell grows is their ability to evade apoptosis which is a cellular programme that eliminates damaged or abnormal cells. Apoptosis occurs through a pathway that lead to the activation of cysteine proteases called caspases responsible for organised dismantling of cells. An impairment of death receptor signalling pathway, unbalanced pro-apototic and anti-apototic proteins, reduced expression of caspases, increased expression of inhibitors of apoptosis (IAP's) leads to uncontrolled cell division that promotes tumour formation and progression and also resistance to treatment [18-20]. Thus by inducing apoptosis, cancer cells can be eliminated. In this study, we therefore evaluated whether CAu, CAm and CCa can induce apoptosis of HeLa and SAS cells. We monitored whether treatment with ethyl acetate fraction of CAu, CAm and CCa caused activation of caspases 3, 8 and 9, we also evaluated Cdk1 and p53 levels which are involved in apoptotic signalling.

RESULTS

Comparative study of compounds present in ethyl acetate fraction of *C. angustifolia*, *C. amada* and *C. caesia* using liquid chromatography-electrospray ionization high-resolution mass spectrometry: *The metabolites present in the ethyl acetate fraction of the three curcuma species were identified by comparing the compounds listed in databases KNApSAcK (http://kanaya.naist.jp) and chemical database – Dictionary of Natural Products (http://dnp.chemnetbase.com) and also as reported in previous articles [21-29]. Compounds which have not been reported yet in the Zingiberaceae family were only given the molecular formula generated. From the LC-HRMS profiles it was found that only Palmitic acid was present in all the three species. Two compounds with molecular formulae* $C_{15}H_{22}O_2$ *(Curcumanolide A) and* $C_{19}H_{20}O_5$ *eluting at retention time 7.9 min and 10.14 min respectively was found in both* C. angustifolia *and* C. caesia*. Compound with molecular formulae* $C_{14}H_{30}O_8$ *eluting at 14.2 min was found in* C. angustifolia *and* C. amada *and* $C_{23}H_{46}O_9$ *eluting at 22.67 min was found in* C. amada *and* C. caesia. *Most of the compounds in* C. angustifolia *and* C. caesia *are sesquiterpenes whereas most compounds in* C. amada *are diarylheptanoids and polyphenols. Zerumin and its isomers were relatively higher that other compounds in* C. angustifolia*, Curcumin I in* C. amada, *Cucumenol or its isomers and* $C_{23}H_{46}O_9$ *in* C. caesia. *Different derivatives of curcumin are present in the ethyl acetate fraction of the three species (Table 1-3).*

Table 1 Compounds present in ethyl acetate fraction of *Curcuma angustifolia*

Peak No	RT (min)	Observed m/z		Calculated m/z		Δ (ppm)	Molecular Formula [MF]	Compound Name
		$[M-H]^-$	$[M + H]^+$	$[M-H]^-$	$[M + H]^+$			
1	6.11		235.1704		234.162	4.86	C15H22O2	Epiprocurcumenol
2	6.69		219.1747		218.1671	1.63	C15H22O	Ar-Turmerol
3	7.9		235.1703		234.162	4.44	C15H22O2	Curcumanolide A
4	8.06	251.1655		252.1731		-1.56	C15H24O3	Zedoarondiol
5	8.41		253.1812		252.1725	4.66	C15H24O3	Curcumadiol
6	8.52	251.1649		252.1731		-1.56	C15H24O3	Isozedoarondiol
7	9.35		235.1712		234.162	8.26	C15H22O2	13-Hydroxygermacrone
8	10.14	327.1249		328.1316		3.28	C19H20O5	
9	10.27		281.1406		280.1311	-1.25	C15H20O5	Linoleic acid
10	11.13	331.1913		332.1993		-0.63	C20H28O4	Hedychilactone C
11	11.23		235.1704		234.162	4.86	C15H22O2	Isocurcumenol
12	11.49	349.2023		350.2099		0.65	C20H30O5	8beta,17-Epoxy-3beta,7beta-Dihydroxy-12(E)-labden-16,15-olide
13	11.62		235.1707		234.162	4.86	C15H22O2	Procurcumenol
14	11.7	335.2232		336.2306		1.17	C20H32O4	
15	11.97	333.2085		334.215		4.02	C20H30O4	4 alpha-methylandrostane-2,3-diol-17-dione
16	12.01		235.1702		234.162	4.01	C15H22O2	Curcumanolide B

17	**12.55**	**305.2143**		**306.2219**		**0.71**	**C22H26O**	**Xanthinin**
18	**12.55**		**235.1714**		**234.162**	**9.12**	**C15H22O2**	**Curcumadione**
19	**12.55**		**257.1529**		**256.1463**	**-2.75**	**C17H20O2**	
20	**13.17**		**235.1711**		**234.162**	**7.84**	**C15H22O2**	**Germacrone-4, 5-epoxide**
21	**13.63**	**317.2127**	**319.2281**	**318.22**		**1.43**	**C20H30O3**	**Zerumin A**
22	**13.82**	**305.2119**		**306.1989**		**3.55**	**C22H26O**	**Xanthumin**
23	**14.27**	**325.1847**		**326.1946**		**-4.96**	**C14H30O8**	
24	**14.65**	**325.1846**		**326.1946**		**-4.96**	**C14H30O8**	
25	**14.84**		**235.1704**		**234.162**	**4.86**	**C15H22O2**	**Curcumenol**
26	**14.89**	**337.1091**	**339.1239**	**338.116**		**-1.69**	**C20H18O5**	**Curcumin II**
27	**15.28**		**303.1975**		**302.1882**	**6.69**	**C19H26O3**	**Dehydro[8]-shogaol**
28	**15.74**		**237.1884**		**236.1776**	**8.83**	**C15H24O2**	**Curcumol**
29	**15.76**	**333.2095**		**334.215**		**4.02**	**C20H30O4**	**Zerumin B**
30	**16.24**		**237.187**		**236.1776**	**8.83**	**C15H24O2**	**Curdione**
31	**18.85**	**255.2343**		**256.2408**		**-3.04**	**C16H32O2**	**Palmitic acid (n-hexadecanoic acid)**
32	**19.93**		**319.2293**		**318.2195**	**7.92**	**C20H30O3**	**Galanal A**
33	**21.14**		**279.1609**		**278.1518**	**6.5**	**C16H22O4**	**Isobutyl phthalate**
34	**21.83**		**301.2188**		**300.2089**	**2.59**	**C20H28O2**	**Mioganal**
35	**22.01**	**317.2135**		**318.22**		**3.95**	**C20H30O3**	**(E)-5-[(1S,4aS,8aS)-5,5,8a-trimethyl-2-methylidene-3,4,4a,6,7,8-hexahydro-1H-naphthalen-1-yl]-**

								3-formylpent-3-en oic acid
36	**22.49**	**465.086**		**466.0964**		**-4.55**	**C17H22O15**	
37	**23.35**		**331.284**		**330.277**	**-0.86**	**C19H38O4**	**Glyceryl palmitate**

Table 2 Compounds present in ethyl acetate fraction of *Curcuma amada*

Peak No.	**RT (min)**	**Observed m/z**		**Calculated m/z**		**Δ (ppm)**	**Molecular Formula [MF]**	**Compound Name**
		$[M - H]^-$	**$[M + H]^+$**	**$[M-H]^-$**	**$[M + H]^+$**			
1	**2.12**		**203.0544**		**202.0477**	**-3.03**	**C8H10O6**	
2	**2.81**		**275.1108**		**274.1053**	**-6.29**	**C12H18O7**	
3	**3.67**		**251.0883**		**250.1569**	**0.12**	**C15H22O3**	**Procurcumadiol**
4	**4.63**		**281.0999**		**280.0947**	**-7.34**	**C14H16O6**	
5	**5.34**		**191.0717**		**190.063**	**3.82**	**C11H10O3**	
6	**5.84**		**265.1049**		**264.0998**	**-8.11**	**C14H16O5**	**1'-Acetoxyeugenol acetate**
7	**6.31**		**195.1015**		**194.0943**	**-0.36**	**C11H14O3**	**Zingerone**
8	**6.57**		**177.0909**		**176.0837**	**-0.6**	**C11H12O2**	**Lachnophyllum ester**
9	**7.11**		**195.1025**		**194.0943**	**4.76**	**C11H14O3**	**3-(4-Hydroxy-3-methoxyphenyl)-2-propenoic acid**
10	**7.68**		**355.175**		**354.1679**	**-0.36**	**C18H26O7**	**Monodemethylcurcumin**
11	**8.03**	**375.1461**		**376.1528**		**4.38**	**C20H24O7**	

12	8.24		207.1023		206.0943	3.52	C12H14O3	Ethyl para-methoxycinnamate
13	8.69	329.2331		330.2412		-3.55	C18H34O5	
14	9.14		427.1752		426.1679	0.16	C24H26O7	
15	9.43		457.186		456.1784	0.67	C25H28O8	
16	10.75		209.1186		208.1099	3.73	C12H16O3	[1]-Paradol
17	11.46		583.1958		582.189	-2.16	C34H30O9	Sophoraflavanone H
18	12.12	367.1181	369.1339	368.1265	368.126	-0.37	C21H20O6	Cyclocucrumin
19	12.81	265.1473		266.1524		-1.34	C15H22O4	5,8-Dihydroxy-3,5,8-trimethyl-4a,5,6,7,7a,8,9,9a-octahydroazuleno[6,5-b]furan-2(4h)-one
20	13.03		543.2033		542.1941	3.6	C32H30O8	
21	13.47	311.1696		312.179		-3.42	C13H28O8	
22	13.52	353.1405			352.1311	6.09	C21H20O5	1,7-bis(4-hydroxy-3-methoxyphenyl)-1,4,6-heptatrien-3-one
23	14.07	191.1081			190.063	3.82	C11H10O3	
24	14.2	325.1857		326.1946		-1.89	C14H30O8	
25	15.03	367.1194	369.1337	368.1265	368.126	1.18	C21H20O6	Curcumin 1
26	15.56	587.2276		588.2365		-0.99	C34H36O9	Cassumunin B
27	15.7		441.1939		440.1894	-6.24	C18H32O12	Nonioside D
28	16.63	557.2217		558.2318		-3.21	C26H38O13	6,12-Tetradecadiene-8,10-diyne-1,5,14-triol; (5S,6E,12E)-form,

								5,14-Di-O-β-D-glucopyranoside
29	**16.84**	**587.2318**	**589.2487**	**588.2424**	**588.2418**	**-0.65**	**C27H40O14**	**Amritoside B**
30	**17.32**	**557.2217**		**558.2254**		**-3.97**	**C26H38O13**	**6,12-Tetradecadiene-8,10-diyne-1,5,14-triol; (5S,6E,12E)-form, 5-O-[β-D-Glucopyranosyl-(1→2)-β-D-glucopyranoside]**
31	**18.42**	**557.2168**		**558.2254**		**-1.46**	**C33H34O8**	
32	**18.82**	**255.2327**		**256.2408**		**0.86**	**C16H32O2**	**Palmitic acid (n-hexadecanoic acid)**
33	**19.24**		**367.192**		**366.1831**	**4.4**	**C23H26O4**	
34	**20.81**		**559.2348**		**558.2254**	**3.85**	**C33H34O8**	**Cassumunarin A**
35	**21.22**	**485.3065**		**486.3139**		**1.76**	**C33H42O3**	
36	**21.65**	**465.3059**		**466.3147**		**4.86**	**C23H46O9**	
37	**21.8**		**411.2181**		**410.2093**	**3.65**	**C25H30O5**	
38	**22.62**	**465.3093**		**466.3147**		**4.86**	**C23H46O9**	

Table 3 Compounds present in ethyl acetate fraction of *Curcuma caesia.*

Peak No	**RT (min)**	**Observed m/z**		**Calculated m/z**		**Δ (ppm)**	**Molecular Formula [MF]**	**Compound Name**
		$[M-H]^-$	**$[M+H]^+$**	**$[M-H]^-$**	**$[M+H]^+$**			
1	**2.78**		**303.1213**		**302.1154**	**-4.62**	**C17H18O5**	
2	**3.39**	**221.0817**		**222.0898**		**1.09**	**C12H14O4**	**2,4,5-Trimethoxycinnamaldehyde**
3	**3.47**		**205.0867**		**204.0786**	**3.8**	**C12H12O3**	

4	**5.47**		**245.1178**		**244.1099**	**2.36**	**C15H16O3**	
5	**6.15**		**281.139**		**280.1311**	**2.31**	**C15H20O5**	**Zedoalactone B**
6	**6.18**	**281.1396**		**282.1473**		**2.22**	**C15H22O5**	**Zedoarolide B**
7	**6.57**		**281.1396**		**280.1311**	**4.45**	**C15H20O5**	**Zedoalactone D**
8	**7.08**		**267.1604**		**266.1518**	**4.92**	**C15H22O4**	**Zedoalactone A**
9	**7.42**		**265.1447**		**264.1362**	**4.77**	**C15H20O4**	**Curcolonol**
10	**7.66**		**267.1602**		**266.1518**	**4.17**	**C15H22O4**	**Zedoalactone C**
11	**7.9**		**235.1716**		**234.162**	**3.16**	**C15H22O2**	**Curcumanolide A**
12	**8.29**	**325.1657**		**326.1735**		**1.57**	**C17H26O6**	**6-Gingesulfonic acid**
13	**8.29**		**267.1616**		**266.1518**	**4.92**	**C15H22O4**	**[4]-Gingerol**
14	**8.85**	**287.0558**		**288.0639**		**0.57**	**C15H12O6**	
15	**8.82**		**267.161**		**266.1518**	**4.92**	**C15H22O4**	**[4]-Isogingerol**
16	**9.22**		**229.1228**		**228.115**	**2.16**	**C15H16O2**	**Curzeone**
17	**9.51**	**391.1769**		**392.1841**		**2.93**	**C21H28O7**	
18	**9.51**		**357.1715**		**356.1624**	**5.18**	**C21H24O5**	**Gingerenone A**
19	**10.09**		**373.1672**		**372.1573**	**7.06**	**C21H24O6**	**Tetrahydrocurcumin**
20	**10.14**	**327.126**		**328.1316**		**4.2**	**C19H20O5**	
21	**10.5**		**515.3029**		**514.2931**	**4.99**	**C30H42O7**	
22	**10.77**		**233.1556**		**232.1463**	**6**	**C15H20O2**	**Curcumafuranol**
23	**11.08**		**679.3128**		**678.304**	**2.22**	**C38H46O11**	
24	**11.11**	**655.313**	**657.3281**	**656.3202**	**656.3197**	**1.2**	**C36H48O11**	**Chisonimbolinin A**
25	**11.27**		**357.1714**		**356.1624**	**4.9**	**C21H24O5**	**1,7-bis(4-hydroxy-3-methoxyphenyl)**

								hept-4-en-3-one
26	**11.28**	**373.1667**		**374.1735**		**1.37**	**C21H26O6**	**Hexahydrocurcumin**
27	**11.53**		**515.302**		**514.2931**	**3.24**	**C30H42O7**	
28	**11.54**	**573.3063**		**574.3147**		**-1.27**	**C32H46O9**	
29	**12.49**	**263.1294**	**265.1446**	**264.1367**	**264.1362**	**1.11**	**C15H20O4**	**Zedoarofuran**
30	**13.54**	**311.1703**		**312.179**		**-3.1**	**C13H28O8**	
31	**13.54**		**231.1394**		**230.1307**	**4.52**	**C15H18O2**	**Curzerenone**
32	**14.01**	**325.1857**		**326.194**		**-1.89**	**C14H30O8**	
33	**14.27**		**497.2904**		**496.2825**	**1.28**	**C30H40O6**	
34	**14.85**		**235.171**		**234.162**	**3.16**	**C15H22O2**	**Curcumenol**
35	**15.52**		**481.2959**		**480.2876**	**2.18**	**C30H40O5**	
36	**17.04**		**229.1239**		**228.115**	**2.16**	**C15H16O2**	**Curzeone**
37	**17.37**		**233.1549**		**232.1463**	**1.69**	**C15H20O2**	**Furanogermenone**
38	**18.16**		**231.1382**		**230.1307**	**1.05**	**C15H18O2**	**5-epi-Curzerenone**
39	**18.86**	**255.2341**		**256.2408**		**4.77**	**C16H32O2**	**Palmitic acid**
40	**18.99**			**479.2839**	**478.2778**	**-4.33**	**C23H42O10**	
41	**19.42**		**235.171**		**234.162**	**3.16**	**C15H22O2**	**Zerumbone epoxide**
42	**20.77**		**477.2633**		**476.2563**	**-0.53**	**C30H36O5**	
43	**21.27**		**149.0236**		**148.016**	**1.88**	**C8H4O3**	
44	**22.67**	**465.3093**		**466.3089**		**2.45**	**C30H42O4**	

In vitro free radical scavenging activity of ethyl acetate fraction of *C. angustifolia*, *C. amada* and *C. caesia*: The free radical scavenging activity of CAu, CAm and CCa was assayed by their reactivity toward free radical DPPH, free radical $ABTS^{\bullet+}$, $NO^{\bullet}$, $O_2^{\bullet-}$. The IC_{50} values

representing the concentration of extract that were able to scavenge 50 % of the free radical were calculated and represented in Figure 1. All three curcuma species showed free radical scavenging activity. *C. amada* was most efficient followed by *C.caesia* (Figure 1).

Cytotoxicity effect of ethyl acetate fraction *C. angustifolia, C. amada and C. caesia* by 3-(4,5-dimethylthiazol-2-yl)-2,5-diphenyl-2H-tetrazolium bromide (MTT) assay: The cytotoxic effect of C. angustifolia, *C. amada* and *C. caesia* was carried out in HeLa and SAS cells. *C. amada* (CAm) was most effective in inhibiting proliferation of both HeLa and SAS cells and a 50 % inhibition (IC_{50}) was at a dose of 275 µg/mL and 156 µg/mL respectively, followed by *C. caesia* (CCa) and C. agustifolia (CAu) (Figure 2; A-HeLa and B-SAS). The IC_{50} doses of the extracts were used in all other assays.

Morphological obsevation by fluorescence microscopy: There is a substantial reduction in the number of viable cells after treatment with all three extracts. Morphologically the cells are shrunken with irregular shape and structure. The nucleus appeared condensed with blebbing of membrane and fragmentation of nuclear material (marked with arrow) were also observed. These morphological changes were not observed in control cells and the nuclei were homogeneously stained (Figure 3).

Cell apoptosis assay using Annexin V-fluorescein isothiocyanate/Propodium Iodide: The Annexin V-FITC/PI apoptosis assay showed that treatment with IC_{50} doses of CAu, CAm and CCa for 48 h induced apoptosis in HeLa cells where 50-60 percent of the cells were in late apoptosis state (Figure 4A), whereas most of the population of SAS cells were in necrotic state and few in late apoptotic state (Figure 4B).

Western blotting assay: p53 and Cdk1 levels were analysed in cell lysate by western blotting after the cells were treated with the extracts CAu, CAm and CCa for 24 h. Equal amounts of proteins were separated by SDS–PAGE, transferred to NCM membrane and immunoblotted with antibodies against p53, Cdk1 and GAPDH. The level of p53 and Cdk1 were normalised to GAPDH. p53 in SAS cells was upregulated after treatment with all the extracts whereas in HeLa cells CAu was not able to cause this effect. Similarly all the three extracts were able to downregulate Cdk1 in SAS cells as well as HeLa cells (Figure 5).

Immunofluorescence of caspase-8, caspase-9 and caspase-3 after treatment with *C. angustifolia, C. amada* and *C. caesia:* The apoptotic effect of CAu, CAm and CCa were furthered assayed by immunoflourescence staining. After the cells were fixed, they were incu-

bated with primary antibody against caspase-8, caspase- 9 and caspase- 3, Alexa fluor 488 - conjugated IgG was used as the fluorescent probe. After 24 h of treatment with CAu, CAm or CCa, some of the cells have loss attachment and are not viable thereby reducing the number of cells considerably. Treated cells displayed overall significant increase in fluorescence intensity compared to their respective untreated control cells indicating cytoplasmic and perinuclear accumulation of detectable amounts of activated caspases. Nuclei staining with Hoechst (blue) indicated that the cells are undergoing events of apoptosis with condensed nucleus, and some with fragmented nuclei (marked with yellow arrow). A corresponding increase in fluorescence intensity of all caspases was observed in cells with such nuclear changes. The fluorescence intensity of caspase-8 was higher than caspase-9 in HeLa cells whereas in SAS cells the intensity is equally comparable for both caspase-8 and 9 (Figure 6 IA, IB and Figure 7 IIA, IIB). The fluorescence intensity of caspase-3 was higher in SAS cells than HeLa cells indicating that its activation is contributed by both caspase 8 and 9 (Figure 8 IIIA, IIIB).

DISCUSSION

Secondary metabolites are synthesized by plants in response to environmental stress and they act as defence mechanism against infections as well as predators [30]. Though the metabolite profile from these plants are expected to have major similarities since they belong to the same genus Curcuma, our results however revealed that only one or two compounds are the same in either of the two species. Compounds $C_{19}H_{20}O_5$ and $C_{15}H_{22}O_2$ are present in both *C. agustifolia* and *C. caesia,* $C_{14}H_{30}O_8$ was found in *C. angustifolia* and *C. amada* and $C_{23}H_{46}O_9$ was found in *C. amada* and *C. caesia.* Few compounds maybe present as isomeric forms in all the three species. The metabolites in *C. augustifoloia* and *C. caesia* are terpenoids and the majority of which are sequiterpenes. Terpenoids are reported to have many biological roles as anticancer, antimicrobial, cytotoxic, antioxidants, anti-inflammatory, and analgesic activities. Zerumin and its isomers which are the major component of *C. angustifolia* are diterpenoids. Zerumin B has been reported to exhibits cytotoxic activity against HL-60, HepG2, MCF-7 and DU-145 cell lines whereas Zerumin A, its isomer have been reported to have angiogenic property in a zebra fish model [31,32]. Compounds with relatively higher abundance than others such as Curcumol, Curdione, Curcumenol and its isomers are also present in *C. angustifolia*. Curcumol have been reported to have anticancer activity by targeting MAPK/ERK, PI3K/Akt and NF-κB signalling pathways [33-36]. Curdione have been reported to inhibit CYP3A4 activity in Caco-2 cells, it reverted liver fibrosis in mice by targeting the TGF-β

pathway and inhibiting oxidative stress [37,38]. Zhang et al. [39] in their studies reported that Curcumenol induced cell death and suppressed cell proliferation in lung cancer cells through ferroptosis. Its isomer, Isocurcumenol was found to inhibit the proliferation of Daltons Lymphoma Ascites (DLA), lung Carcinoma (A549), nasopharyngeal carcinoma (KB), leukemic (K562) cells [40]. Curcumenol and its isomers were also reported to exhibit antiinflammatory activities [41-44]. The major components in *C. caesia* are Curcumenol and $C_{23}H_{46}O_9$ followed by Gingerol and Furanogermenone. Gingerol has been found to possess anticancer activities by inducing apoptosis, regulating cell cycle and inhibiting angiogenesis [45]. Curcumin I, a diarylhepatanoid is the major component of *C. amada*. Curcumin have been extensively studied and reported for its anticancer properties. Curcumin also increases the effectiveness of chemotherapy and radiotherapy [46-49].

p53 is a tumour suppressor that functionally promotes apoptosis and prevents damage cells from progressing through the cell cycle thereby preventing oncogenic transformation and tumour progression. p53 is a regulator of transcription which regulates genes involved in cell cycle such as p21 and 14-3-3σ. p53 also regulates apoptosis-related genes such as the Bcl-2 family members, tumour necrosis factor receptor (TNFR) family of death receptors, IGF-BP3, PTGF-beta, and PERP, which are responsible in promoting apoptosis. Whether a cell will undergo apoptosis or cell cycle arrest is dependent on the p53 protein levels and cellular environment. A high p53 proteins level directs the cell to undergo apoptosis [50-52]. In our study, we evaluated the p53 levels in HeLa and SAS cells post 24 h treatment with *C. angustifolia*, *C. amada* and *C. caesia* to understand the mechanism of apoptosis induced by the three different curcuma species. After SAS cells were treated with CAu, CAm and CCa, p53 was upregulated, whereas only CAm and CCa caused an upregulation of p53 in HeLa cells.

Cyclin-dependent kinases (CDKs) are mammalian heterodimeric serine/threonine protein kinases. Cdk1 and Cdk2 play an important role in the cell division cycle and are master regulators of DNA damage checkpoint and repair pathways and they have also been reported to play a role in apoptosis [53-55]. Post treatment with the extracts caused a downregulation of Cdk1 in both cells.

We also evaluated caspase 3, 8 and 9 since they are the executioner of many apoptotic pathways. Caspases are cysteine proteases that cleave peptides with an aspartic acid in the P1 position. Caspases are synthesized as inactive proenzymes and are activated by dimerization, proteolytic cleavage through auto-activation or trans-activation process [56-57]. Caspase-8 can

be activated either by a receptor dependent process through the stimulation of death receptors such as CD95, tumour necrosis factor receptor1 (TNF-R1), and TNF-related apoptosis inducing ligand receptors (TRAIL-R1/TRAIL-R2), by direct cleavage through other caspases or proteases like granzyme B and human immunodeficiency virus type 1 protease and also by a post mitochondrial event [58-62]. Caspase-9 activation can be caused by downstream signalling of caspase 8 or through diverse damages or stress signals. In both pathways, the activation of BH3-Bcl-2 interacting protein caused mitochondrial outer membrane permeabilization and release of cytochrome c from the mitochondria. Cytochrome c in turn promotes the assembly of the apoptosome which is a multimeric protein complex of apoptotic protease activating factor 1 (Apaf-1), cytochrome c and the cofactor dATP/ATP. Recruitment of caspase-9 by the apoptosome and its dimerization leads to activation of caspase-9 [63-66]. Caspase-3 can be transactivated by either caspase-8 or caspase-9 or by autoproteolytic cleavage leading to the assembly of the active heterotetrameric enzyme [67,68]. Caspase-3 is one of the key executioner enzymes catalyzing the cleavage of many important proteins such as poly(ADP-ribose)polymerase (PARP), the retinoblastoma protein, protein kinase C (PKC)-gamma and delta, procaspases 2, 6, 7, 9, beta catenin, ICAD to release CAD (Caspase-activated DNase) which causes chromatin condensation and deoxyribonucleic acid (DNA) fragmentation. Cleavage of Gelsolin, an actin binding protein induces cytoskeletal reorganization and disintegration of the cell into apoptotic bodies [69-71]. Our studies showed that treatment of HeLa and SAS cells with all three curcuma species CAu, CAm, and CCa caused activation of caspases 8, 9 and subsequent activation of caspase-3 leading to apoptosis of cells. This is also substantiated by the observable changes in cell and nuclear morphology such as chromatin condensation and fragmentation. Externalization of phosphatidylserine on the surface of apoptotic cells and their fragments and phagocytosis of apoptotic cells is the last event in apoptosis which can be detected by Annexin V FITC/PI flow cytometric analysis [72]. Annexin V is an anticoagulant protein which can bind to phosphatidylserine on the outer leaflet of the cytoplasmic membrane whereas PI intercalates into nucleic acids, PI can permeate the cells only if the plasma and nuclear membranes are compromised [73]. Flow cytometric analysis also confirmed that HeLa and SAS cells were undergoing apoptosis after treatment with CAu, CAm and CCa. SAS cells however, were also found in the necrosis stage; it can be that the cells were undergoing apoptotic process but converted into a necrotic process through an apoptosis-necrosis continuum which can be due to a decrease in the availability of caspases and intracellular ATP after 48 h of treatment [74,75]. Our study suggested that *C. angustifolia*, *C. amada* and *C. caesia* induce apoptosis through a p53 dependent pathway. The two plants

may have induced DNA damage resulting in increased p53 expression and a decreased in Cdk 1. p53 function is also regulated by Cdks and inhibition of multiple Cdks have been shown to activate p53 [76-77]. Curcumin I which is a major component of *C. amada* have been reported to induce DNA damage and increase expression of p53 and other repair associated proteins in HeLa cells [78]. Terpenoids have been demonstrated to act as prooxidant at high concentration whereas at low concentration they act as antioxidants [79]. From the free radical scavenging assay all the plants were able to scavenge the free radicals at very low concentration thereby acting as antioxidants. At the IC_{50} concentration which is a much higher dose, the terpenoids of *C. caesia* act as prooxidants and may have caused DNA damage leading to increased p53 expression. Increased expression of p53 subsequently led to mitochondrial outer membrane permeabilization and activation of the caspase 9 which inturn activates caspase 3 and 8 via the intrinsic pathway. *C. angustifolia* induced apoptosis is p53 independent and may have acted via the extrinsic apoptotic pathway in HeLa cells.

Conclusions

Our results show that there is a variation in the metabolites present in the three curcuma species which play a role in inducing apoptosis of HeLa and SAS cells. *C. angustifolia*, *C. amada* and *C. caesia* caused apoptosis of SAS cells through a p53 pathway whereas *C. angustifolia* may have induced apoptosis via the extrinsic pathway in HeLa cells. The three curcuma species are rich sources of metabolites that have shown to play a role in ameliorating many pathophysiological conditions and are therefore sources of many potential drugs or complimentary medicines.

MATERIALS AND METHODS

Reagents: Dulbecco's Modifed Eagle's Medium (DMEM), fetal bovine serum (FBS), Antibiotic Antimycotic Solution (100×) and all other cell culture reagents, Bovine Serum Albumin (BSA), 2,2-diphenyl-1-picrylhydrazyl), 2,2-azinobis (3-ethyl benzothiazoline) -6-sulfonic acid, Potassium persulfate, Phenazine methosulfate (PMS), β-Nicotinamide adenine dinucleotide (NADH) , Sodium nitroprusside (SNP), Naphthyl ethylenediamine dihydrochloride, Sulphanilamide, 3-(4,5-dimethylthiazol-2-yl)-2,5-diphenyltetrazolium bromide (MTT), Phosphate buffered saline (PBS), Tris Buffered Saline (TBS), Tris Buffered Saline with 0.1 % Tween-20 (TBST), Tris-Glycine-SDS Buffer 10×, Dimethyl sulfoxide (DMSO), TritonX-100 , Hoechst 33258 solution, 3,3′,5,5′-tetramethylbenzidine (TMB) substrate for membranes,

Amersham™ Protran® Western blotting membrane, nitrocellulose were procured from Sigma-Aldrich (St. Louis, MO, USA). Anti-caspase-3 (E-8), anti-caspase-8 p18 (D-8), anti-caspase-9 (96.1.23), anti-Cdk1/Cdk2 (AN21.2), anti-p53 (DO-1) anibodies were procured from Santa Cruz Biotechnology, Inc. (Santa Cruz, CA, USA), GAPDH, Goat anti-mouse IgG1 conjugated Alexa fluor 488 and Goat anti-mouse IgG conjugated Horse radish peroxidise (HRP) were procured from Thermo Fisher Scientific Inc (Rockford, IL, USA).

Separation of phytochemicals from *C. angustifolia, C. amada* and *C. caesia:* The plant samples were collected at a location of 25°68′ N latitude and 91°93′ E longitude in the state of Meghalaya, India. *Curcuma amada* (voucher specimen 'NEHU-11897') and *Curcuma caesia* (voucher specimen 'NEHU 11927') was identified by Dr. P. B. Gurung, herbarium Curator, Department of Botany, North-Eastern Hill University, Shillong, India. *Curcuma angustifolia* (Barcode: CAL0000191760) was identified by Dr. R. Gogoi, Scientist-F, BSI Sikkim Himalayan Regional Centre, Gangtok, by comparing with known specimen deposited at the herbarium of Botanical Survey of India.

Rhizomes of the three curcuma species were washed, cut, dried at 37-40 °C for 6-8 days and ground into powder. The phytochemicals present were sequentially extracted based on polarity using a Soxhlet apparatus. A ratio of 1: 3 (w/v) samples: solvent was taken. Extraction was first carried out with hexane for 6 h, then ethyl acetate for 6 h, and finally methanol for 6 h. After each extraction, the powder was dried to evaporate the remaining preceding solvent. The filtrate obtained was concentrated by a vacuum evaporator or dried to remove all the solvent. The oils and powdered fractions obtained were stored at 4 °C.

Identifcation and characterization of secondary metabolites of *C. angustifolia, C. amada* and *C. caesia* by Liquid chromatography–high-resolution mass spectrometry: Liquid chromatography–high-resolution mass spectrometry (LC-HRMS) was used for comparative analysis of metabolites in ethyl acetate fraction of CAu, CAm and CCa. Samples were prepared in methanol (0.5 mg/mL), filtered through a 0.22-µm polyvinylidene difluoride (PVDF) syringe filter and separated in an Agilent 1200 HPLC system (Agilent Technologies; Santa Clara, CA, USA). A sample volume of 5 µL was automatically loaded onto a SunFire C18 of column size 250 mm × 4.6 mm, 5 µm. The composition of the mobile phase was 5 mM ammonium acetate buffer (A) and acetonitrile (B). The flow rate of was set at 1.5 mL/min and the fol-

lowing solvent gradient was used for separation and elution of compounds- 5% B (0-6 min), 30% B (6-12 min), 60% B (12-20 min), 80% B (20-26 min) and 5% B (26-30 min). The separated compounds was analysed in Agilent G6510A Accurate-Mass Quadrupole Time-of-Flight (Q-TOF). The ion source is dual ESI, capillary temperature is at 340 °C, nebulizer pressure at 40 psi and gas flow rate was 11 L/min. The ion source parameters VCap, fragmentor, skimmer1, and octapole radio frequency (RF) peak voltages were set to 3500 V, 175 V, 65 V, and 750 V respectively. The mass range of m/z 100–2000 and resolving power above 15,000 full widths at half maximum was set as detection parameter [80]. The exact mass calculation and prediction of chemical formula was carried out using The ISIC- EPFL mstoolbox (https://ms.epfl.ch)

In vitro* free radical scavenging activity of *C. angustifolia, C. amada* and *C. caesia: The ability to scavenge free radicals such as DPPH (2,2-diphenyl-1-picrylhydrazyl), $ABTS^{\bullet+}$ (2,2-azinobis (3-ethyl benzothiazoline)-6-sulfonic acid), superoxide ($O_2^{\bullet-}$) and nitric oxide ($NO^{\bullet}$) by the three curcuma species were assayed spectrophotometrically using Termo Scientific Multiskan FC microplate photometer, USA. A concentration ranging from 0.0625 mg/mL to 1 mg/mL of sample was used in each assay. The amount of sample that decreased the initial absorbance by 50 % (IC_{50}) indicates the scavenging activity of that sample. For DPPH, the reaction mixture contained 100 µM DPPH and 20 µL sample incubated at room temperature (r.t) and absorbance was read at 517 nm after 30 min. ABTS stock solution (1.1 mg/mL) was allowed to react with 2.45 mmol Potassium persulfate in the dark for 6 h at r.t to produce ABTS radical cation ($ABTS^{\bullet+}$). Samples of 100 µl was added to 150 µl of the $ABTS^{\bullet+}$ and the absorbance was measured immediately after 5 min at 734 nm. For superoxide radical scavenging activity, 100 µL sample was added to a reaction mixture containing phosphate buffer (100 mmol, pH 7.4), NBT (156 µM), Phenazine methosulfate (PMS) (60 µM), β-Nicotinamide adenine dinucleotide (NADH) (73 µM). The absorbance was read at 560 nm after 5 min incubation at r.t. $NO^{\bullet}$ scavenging activity was quantified by incubating 100 µL sample with a reaction mixture containing 10 mmol aqueous sodium nitroprusside (SNP) and phosphate buffered saline (PBS; pH7.4) at r.t for 150 min. After incubation, Griess reagent (1% w/v sulphanilamide, 0.1% w/v naphthyl ethylenediamine dihydrochloride in 25% phosphoric acid) was added and again incubated at r.t for 30 min. The absorbance was measured at 546 nm [80].

Cell lines: HeLa cell line was obtained from the National Centre for Cell Science (NCCS), National Repository for cell lines in India. SAS cell line was gifted to Dr. Kekungu-u Puro by

Dr Sachin Kumar, Department of Biosciences and Bioengineering, Indian Institute of Technology Guwahati, India [81].

Cell viability assay: HeLa cells and SAS cells were cultured as monolayer in Dulbecco's Modifed Eagle's Medium (DMEM), containing 10 % fetal bovine serum, 10 mg/mL penicillin/streptomycin and 25 µg/mL amphotericin B. The cells were placed in a 5 % CO_2 incubator and grown at 37 °C. Exponentially growing cells were seeded in 96-well plates (1.5×10^3 cells/well) and grown for 24 h. Cells were then treated with test samples (ethyl acetate fraction of CAu, CAm, CCa at concentration range of 1 mg/mL - 0.0625 mg/mL) prepared in DMEM containing 0.5 % dimethyl sulfoxide (DMSO). Cells treated with DMEM and 0.5 % DMSO served as a control group. After 48 h of treatment, the media was removed and 20 µL of [4, 5- dimethylthiazol -2- yl] -2,5 - diphenyltetrazolium bromide (MTT) at a concentration of 5 mg/mL was added to each well and incubated at 37 °C for 4 h. DMSO (100 µl) was added and incubated for 30 min to solubilized the MTT-formazan complex formed. The absorbance of the contents was measured at 570 nm. The inhibition of each test sample was calculated and IC_{50} for each extract was extrapolated from the graph. The IC_{50} concentration of each extract was used for all other experiments [80].

Apoptosis assay using Annexin V-fluorescein isothiocyanate/Propodium Iodide: The apoptotic effect of CAu, CAm and CCa was assayed using the BD LSRFortessa™ cell analyzer. A cell density of 0.1×10^6 cells/well was seeded in 24-well plates and grown for 24 h. They were then treated with test samples at their IC_{50} concentration for 48 h. The cells were collected and washed twice with PBS. Annexin V/PI (AV/PI) double staining was carried out according to manufacturer instructions provided in Apoptosis Detection Kit PF032 (Calbiochem) [80].

Changes in nuclear morphology using Hoechst staining: Cells were seeded at a density of 0.3×10^6 on coverslips surface placed in 6 wells plates. Treatment was carried out as described earlier. After 48 h treatment, cells were fixed in 90 % ethanol for 5 min at room temperature (r.t). Cells were then washed with PBS thrice and stained with Hoechst 33342 for 15 min at r.t in dark, mounted in slides using glycerol: PBS (1:1) mountant and viewed under Axio Zeiss Vert A1 microscope (Carl Zeiss, Oberkochen, Germany) at ×10 and photographed [80].

Immunofluorescence detection of caspases 8, 9 and 3: Cells were seeded at a density of 0.3×10^6 in 6 wells plates and grown for 24 h. Cells were treated with CAu, CAm and CCa at IC_{50}

doses for 24 h, after which, cells were rinsed with cold PBS twice. The cells were then fixed with chilled methanol for 10 min and air dry. Fixed cells were permeabilized and blocked in blocking buffer (5 % BSA and 0.25 % TritonX-100 in PBS) for 30 min at room temperature. Cells were then washed with PBS and incubated with primary antibodies (1:100) diluted in PBS and and 1.5 % blocking buffer overnight at 4˚C. After washing with PBS three times (5 min/wash), cells were incubated with PE -conjugated goat anti-mouse IgG antibody at room temperature for 1 h. Cells were washed with PBS thrice followed by nuclear counter-staining with Hoechst 33342 for 15 min (Elwakeel et al. 2021)[55]. The cells were washed again with PBS and were examined under Axio Zeiss Vert A1 microscope at x 20 and photograph. The images were analyzed using ImageJ 1.51 software (National Institutes of Health, Bethesda, MD, USA).

Protein extraction and western blot analysis: Cells were seeded in a 25 cm^2 at a density of 0.7 x 10^6 and grown for 24 h at 37˚C. Treatment with CAu, CAm and CCa was carried out for 24 h. Extracts were discarded and cells were collected and washed with PBS twice. Cells lyses was carried out using RIPA lysis buffer and 10 mM phenylmethylsulfonyl fluoride and incubated for 1 h. Cell lysates were centrifuged at 20,000 x g for 15 min. The supernatant was collected and total protein was quantified by Bradford method. Protein samples (60-80 µg) from untreated control and each treatment group were loaded into separate wells and electrophorectic separation of proteins was carried out in 10 % SDS-Poly Acrylamide Gel Electrophoresis (SDS-PAGE). The separated proteins were transferred onto Nitrocellulose membranes. The membranes were incubated in blocking solution (5 % non-fat milk in TBS) for 1 h at r.t. Specific primary antibodies (1:200), were added and incubated overnight at 4˚C. The membranes were washed three times with TBST solution and were then incubated with the secondary antibodies (1: 1,000) in 5 % non-fat milk in TBS. After secondary antibody incubation, the membranes were washed three times with TBST and the proteins were detected using HRP substrate (Sigma) [55]. Band intensity was analyzed using ImageJ 1.51 software (National Institutes of Health, Bethesda, MD, USA).

The research proposal and the above methods were carried out in accordance with the proposal submitted which was approved by the University Grants Commission, Government of India.

Statistical analysis

The data are presented as the means ± standard deviation. All of the statistical analyses were performed using GraphPad Prism 5 Sofware (GraphPad Sofware, Inc., USA). Statistical comparisons between the control and treatment groups were conducted using one-way analysis of variance followed by Dunnett's multiple comparisons test. A $P<0.05$ was considered to indicate a statistically signifcant difference.

Limitations of the study:

i) As mentioned in the results, some compounds in each of the plant species were only given the molecular formula generated. Further characterization of these compounds can be carried out through MS/MS analysis or by NMR. ii) Though there are reports of the anticancer activity of some of these compounds as mentioned in the discussion we are unable to isolate individual compounds at this point and assess their anticancer property individually.

Acknowledgments: We thank Sophisticated Analytical Instrument Facility, Central Drug Research Institute, Lucknow, India, for LC-HRMS.

Ethics Statement and Regulatory Compliance: Informed consent was Not Applicable. The authors declare that all field research, specimen collection, and sampling protocols carried out for this study were conducted in strict accordance with the IUCN Policy Statement on Research Involving Species at Risk of Extinction**.**

Funding Declaration

"This research was funded and approved by University Grants Commission, Government of India under the UNIVERSITY GRANTS COMMISSION: Post-Doctoral Fellowship for SC/ST Candidates for the year 2016-17 under Grant No. F./PDFSS-2015-17MEG--12845."

Conflict of Interest Statement: "The authors declare no conflict of interest."

Data availability statement: All data generated or analysed during this study are included in this published article and its supplementary information files.

References

1. Sung, H.; Ferlay, J; Siegel, R. L.; Laversanne, M.; Soerjomataram, I.; Jemal, A.; Bray, F. Global cancer statistics 2020: GLOBOCAN Estimates of incidence and mortality worldwide for 36 cancers in 185 countries. *CA Cancer J Clin* **2021**, 71, 209–249.

2. Mathur, P.; Sathishkumar, K.; Chaturvedi, M.; Das, Priyanka; Sudarshan, K. L.; Santhappan, Stephen; Nallasamy, V.; John, A.; Narasimhan, S.; Roselind, F. S.; on behalf of ICMR-NCDIR-NCRP Investigator Group. Cancer Statistics, 2020: Report from National Cancer Registry Programme, India. *JCO Glob Oncol* **2020**, 6, 1063-1075.

3. Institute of Medicine (U.S.). Committee on the Use of Complementary and Alternative Medicine by the American Public. *Complementary and Alternative medicine in the United States*. The National Academies Press, Washington (DC), U.S., 2005.

4. Stub, T.; Quandt, S.A.; Arcury, T.; Sandberg, J. C.; Kristoffersen, A. E. Conventional and complementary cancer treatments: where do conventional and complementary providers seek information about these modalities? *BMC Health Serv Res* **2018**, 18, 854.

5. Jermini , M.; Dubois, J.; Rodondi, P.; Zaman, K.; Buclin, T.; Csajka, C.; Orcurto, A.; Rothuizen, L. E. Complementary medicine use during cancer treatment and potential herb-drug interactions from a cross-sectional study in an academic centre. *Sci Rep***2019**, 9, 5078.

6. Knecht, K.; Kinder, D.; Stockert, A. Biologically-based complementary and alternative medicine (CAM) use in cancer patients: The good, the bad, the misunderstood. *Front Nutr* **2020**, 6, 196.

7. World Health Organization 2013. WHO traditional medicine strategy: 2014-2023. World Health Organization.

8. Sarma, J.; Dey, S.; Verma, D. *Curcuma rubrobracteata* (Zingiberaceae): Range extension and new addition to flora of Meghalaya. *Indian J Plant Sci.* **2016**, 5(3), 37-39.

9. Mao, A. A; Sinha, B. K.; Verma, D.; Sarma, N. Check-list of flora of Meghalaya. *Meghalaya Biodiversity Board, Shillong, India,* 2016; pp. 184.

10. Policegoudra, R.S.; Aradhya, S.M.; Singh, L. Mango ginger (*Curcuma amada* Roxb.) - A promising spice for phytochemicals and biological activities. *J Biosci* **2011**, 36(4), 739–748.

11. Sharma, A. Traditional processing of Shotti (*Curcuma angustifolia* Roxb.)- A rhizome based ethnic weaning food. *Indian J Tradit Knowl* **2012**, 11, 154-155.

12. Sahu, R.; Saxena, J. A brief review on medicinal value of *Curcuma caecia*. *Int J of Pharm Life Sci (IJPLS)* **2013**, 4(5), 2664-2666.

13. Das,S.; Mondal ,P.; Zaman, Md. K. *Curcuma caesia* Roxb. and it's medicinal uses: A review. *IJRPC* **2013**, 3(2), 370-375.

14. Hadem, K.L. H.; Sharan, R. N.; Kma, L. Inhibitory potential of methanolic extracts of *Aristolochia tagala* and *Curcuma caesia* on hepatocellular carcinoma induced by di-ethylnitrosamine in BALB/c mice. *J Carcinog* **2014**, 13, 7.

15. Hadem, K.L. H.; Sharan, R.N.; Kma, L. Phytochemicals of *Aristolochia tagala* and *Curcuma caesia* exert anticancer effect by tumour necrosis factor-α-mediated decrease in nuclear factor kappaB binding activity. *J Basic Clin Pharm* **2016**, 7, 1-11.

16. Hadem, K. L. H.; Sen, A. *Curcuma* species: A source of anticancer drugs. *J Tumour Med Prev* **2017**, 1(5), 555572.

17. Sharma, S.; Ghataury, S. K.; Sarathe, A.; Dubey, G.; Parkhe, G. *Curcuma angustifolia* Roxb, (Zingiberaceae): Ethnobotany, phytochemistry and pharmacology: A review. *J Pharmacogn d Phytochem* **2019**, 8(2), 1535-1540.

18. Fulda, S. Evasion of apoptosis as a cellular stress response in cancer. *Int J Cell Biol* **2010**, 370835.

19. Wong, R. S. Y. Apoptosis in cancer: from pathogenesis to treatment. *J Exp Clin Cancer Res* **2011**, 30, 87.

20. Fernald, K.; Kurokawa, M. Evading apoptosis in cancer. *Trends Cell Biol* **2013**, 23(12), 620–633.

21. Geetha Nambiar, M. K. Isolation, structural elucidation and biological properties of secondary metabolites in some plants, University of Calicut, India, 1999; pp. 79-81.

22. Li, S.; Yuan, W.; Deng, G.; Wang, P.; Yang, P.; Aggarwal, B. B. Chemical composition and product quality control of Turmeric (*Curcuma longa* L.). *Pharm Crop* **2011**, 2, 28-54.

23. Kim, M.; Kim, J. S.; Hong, J.; Ji, M.; Lee, Y. Cytotoxic activity of the extracts from *Curcuma zedoaria*. *J Toxicol Pub Health* **2003**, 19(4), 293-296.

24. Afzal, A.; Oriqat, G.; Khan, M. A.; Jose, J.; Afzal, M. Chemistry and Biochemistry of Terpenoids from Curcuma and Related Species. *J Biol Act Prod Nat* **2013**, 3(1), 1-5.

25. Hamdi , O. A. A.; Rahman, S. N. S. A.; Awang, K.; Wahab, N. A.; Looi, C. Y; Thomas, N. F.; Malek, S. N. A. Cytotoxic constituents from therRhizomes of *Curcuma zedoaria*. *Sci World J* **2014**, 321943.

26. Loboa, R.; Prabhua, K. S.; Shirwaikara, A.; Shirwaikar, A. *Curcuma zedoaria* Rosc. (white turmeric): A review of its chemical, pharmacological, and ethnomedicinal properties. *J Pharm Pharmacol* **2009**, 61, 13-21.

27. Simoh, S.; Zainal, A. Chemical profiling of *Curcuma aeruginosa* Roxb. rhizome using different techniques of solvent extraction. *Asian Pac J Trop Biomed* **2015**, 5(5), 412-417.

28. Kamazeri, TSAT; Samah, O.; A.; Taher, M.; Susanti, D.; Qaralleh, H. Antimicrobial activity and essential oils of *Curcuma aeruginosa*, *Curcuma mangga*, and *Zingiber cassumunar* from Malaysia. *Asian Pac J Trop Med* **2012**, 202-209.

29. Lu, J.; Dang, Y.; Huang, M.; Xu, W.; Chen, X.; Wang, Y. Anti-cancer properties of terpenoids isolated from rhizoma *Curcumae* – A review. *J Ethnopharmacol* **2012**, 143, 406–411.

30. Dewick, P.M. Medicinal Natural Products: A Biosynthentic Approach. 2nd ed. West Sussex, UK: John Wiley and Son; 2002, pp. 520.

31. Abas, F.; Lajis, N. H., Shaari, K.; Israf, D. A.; Stanslas, J.; Yusuf, U. K.; Raof, S. M. A labdane diterpene glucoside from the rhizomes of *Curcuma mangga. J Nat Prod* **2005**, 68, 1090-1093.

32. He, Z.; Gilli, C.; Yue, G. G.; Lau, C. B.; Greger, H.; Brecker, L.; Ge, W.; But, P. P. Anti-angiogenic effects and mechanisms of zerumin A from *Alpinia caerulea*. *Food Chem* **2012**, 132, 201–208.

33. Zhang, I.; Su, G.; Tang, Z.; Wang, Li.; Fu, W.; Zhao, S.; Ba, Y.; Bai, B.; Yue, P.; Lin, Y.; Bai, Z.; Hu, J.; Meng, W.; Qiao, L.; Li, X.; Xie, X. Curcumol exerts anti-cancer effect in cholangiocarcinoma cells via down-regulating CDKL3. *Front Physiol* **2018**, 9, 234. doi: 10.3389/fphys.2018.00234.

34. Wei, W., Rasul, A.; Sadiqa, A.; Sarfraz, I.; Hussain, G.; Nageen, B.; Liu, X.; Watanabe, N.; Selamoglu, Z.; Ali, M.; Li, X.; Li, J.Curcumol: From plant roots to cancer roots. *Int J Biol Sci* **2019**, 15(8), 1600-1609.

35. Zang, S.; Tang, Q.; Dong, F.; Liu, H.; Li, L.; Guo, F.; Pan, X.; Lin, H.; Zeng, W.; Cai, Z; Zhong, Q.; Zang, N.; Zang, L. Curcumol inhibits the proliferation of gastric adenocarcinoma MGC-803 cells via downregulation of IDH1. *Oncol Rep* **2017**, 38, 3583-3591.

36. Hashema, S.; Nisara, S.; Sageenab, G.; Machac, M. A.; Yadava, S. K.; Krishnankuttye, R.; Uddine, S.;, Harisa, M.; Bhata, A. A. Therapeutic effects of Curcumol in several diseases; An Overview. *Nutr Cancer* **2021**, 73(2), 181-195..

37. Hou, X.; Hayashi-Nakamura E.; Takatani-Nakase, T.; Tanaka, K.; Takahashi, K.; Komatsu, K.; Takahashi, K. Curdione plays an important role in the inhibitory effect of *Curcuma aromatica* on CYP3A4 in Caco-2 Cells. *EvidBased Complement Alternat Med* **2011**, 913898.

38. Dai, W.; Qin, Q.; Li, Z.; Lin, Li.; Li, R.; Fang, Z.; Han, Y.; Mu, W.; Ren, L.; Liu, T.; Zhan, X.; Xiao, X.; Bai, Z. Curdione and Schisandrin C synergistically reverse hepatic fibrosis via modulating the TGF-b pathway and inhibiting oxidative stress. *Front Cell Dev Biol* **2021**, 9, 763864.

39. Zhang, R.; Pan, T.; Xiang, Y.; Zhang, M.; Xie, H.; Liang, Z.; Chen, B.; Xu, C.; Wang, J.; Huang, X.; Zhu, Q.; Zhao, Z.; Gao, Q.; Wen, C.; Liu, W.; Ma, W.; Feng, J; Sun, X.; Duan, T.; Leung, E. L.; Xie, T.; Wu, Q.; Sui, X. Curcumenol triggered ferroptosis in lung cancer cells via lncRNA H19/ miR-19b-3p/FTH1 axis. *Bioact Mater* **2022**, 13, 23-36.

40. Lakshmi, S.; Padmaja, G.; Remani, P. Antitumour effects of Isocurcumenol isolated from *Curcuma zedoaria* rhizomes on human and murine cancer cells. *Int J Med Chem* **2011**, 253962.

41. Jang, M. K.; Sohn, D. H.; Ryu, J. A curcuminoid and sesquiterpenes as inhibitors of macrophage TNF-a release from *Curcuma zedoaria*. *Planta Med* **2001**, 67, 550-552.

42. Jang, M. K.; Lee, H. J.; Kim, J. S.; Ryu, J. A curcuminoid and two sesquiterpenoids from *Curcuma zedoaria* as inhibitors of nitric oxide synthesis in activated macrophages. *Arch Pharm Res* **2004**, 27(12), 1220-1225.

43. Lo, J.Y.; Kamarudin, M. N. A.; Hamdi, O. A. A.; Awang, K.; Kadir, H. A. Curcumenol isolated from *Curcuma zedoaria* suppresses Akt-mediated NF-κB activation and p38 MAPK signaling pathway in LPS-stimulated BV-2 microglial cells. *Food Funct* **2015**, 6, 3550.

44. Yang, X.; Zhou, Y.; Chen, Z.; Chen, C.; Han, C.; Li, X.; Tian, H., Cheng, X,; Zhang, K.; Zhou T.; Zhao, J. Curcumenol mitigates chondrocyte inflammation by inhibiting the NF-κB and MAPK pathways, and ameliorates DMM-induced OA in mice. *Int J Mol Med* **2021**, 48, 192.

45. Mohd Yusof, Y.A. Gingerol and Its Role in Chronic Diseases. In: *Drug Discovery from Mother Nature. Advances in Experimental Medicine and Biology,* Gupta, S.; Prasad, S.; Aggarwal, B.; Eds.; Springer International Publishing, Switzerland , 2016; Volume 929, pp. 188-191.

46. Vallianou, N. G.; Evangelopoulos, A.; Schizas, N.; Kazazis, C. Potential anticancer properties and mechanisms of action of curcumin. *Anticancer Res* **2015**, 35, 645-652.

47. Allegra, A.; Innao, V.; Russo, S.; Gerace, D.; Alonci, A.; Musolino, C. Anticancer activity of Curcumin and its analogues: Preclinical and clinical studies. *Cancer Invest* **2016**.

48. Tomeh, M. A.; Hadianamrei, R.; Zhao, X. A review of Curcumin and its derivatives as anticancer agents. *Int J Mol Sci* **2019**, 20, 1033.

49. Mansouri, K.; Rasoulpoor, S.; Daneshkhah, A.; Abolfathi ,S.; Salari, N.; Mohammad, M.; Rasoulpoor, S.; Shabani, S. Clinical effects of curcumin in enhancing cancer therapy: A systematic review. *BMC Cancer* **2020**, 20, 791.

50. Bellamy, C. O. C. p53 and apoptosis. *Br Med Bull* **1996**, 3, 522-538.

51. Shen, Y.; White, E. p53-dependent apoptosis pathways. *Adv Cancer Res* **2001**, 82, 55-84.

52. Fridman, J. S.; Lowe, S. W. Control of apoptosis by p53. *Oncogene* **2003**, 22, 9030–9040.

53. Su, C.; Lin, J. , Chen, G.; Lin2, W.; Chung, J. Down-Regulation of Cdc25c, Cdk1 and Cyclin B1 and up-regulation of wee1 by Curcumin promotes human colon cancer Colo 205 cell entry into G2/M-phase of cell cycle. *Cancer Genomics Proteomics* **2006**, 3: 55-62.

54. Zhang, Y.; Ge, Y.; Shi, W.; Hu, C.; Bai, X.; Rong, J.; Yu, M.; Cds-1548 induces apoptosis in HeLa cells by activating caspase 3. *Oncol Lett* **2019**, 18, 1881-1887.

55. Elwakeel, A.; Sari, A.N.; Dhanjal, J.K.; Meidinna, H.N.; Sundar, D.; Kaul, S.C.; Wadhwa, R. Mutant p53L194F harboring luminal-a breast cancer cells are refractory to apoptosis and cell cycle arrest in response to Mortaparibplus, a multimodal small molecule inhibitor. *Cancers* **2021**, 13, 3043.

56. Kruidering, M.; Evan, G. I. Caspase-8 in apoptosis: The beginning of “the end”? *IUBMB Life* **2000**, 50, 85–90.

57. Fulda, S. Caspase-8 in cancer biology and therapy. *Cancer Lett* **2009**, 281, 128–133.

58. Wesselborg, S.; Engels, I. H.; Rossmann, E.; Los M.; Schulze-Osthoff, Klaus. Anti-cancer drugs induce Caspase-8/FLICE activation and apoptosis in the absence of CD95 receptor/ligand interaction. *Blood* **1999**, 93(9), 3053-3063.

59. Engels, I. H.; Stepczynska, A.; Stroh, C.; Lauber, K.; Berg, C.; Schwenzer, R.; Wajant, H.; Janicke, R. U.; Porter, A. G.; Belka, C.; Gregor, M.; Schulze-Ostho, K.; Wesselborg, S. Caspase-8/FLICE functions as an executioner caspase in anticancer drug-induced apoptosis. *Oncogene* **2000**, 19, 4563–4573.

60. Sohn, D.; Schulze-Osthoff K.; Janicke, R. U. Caspase-8 can be activated by interchain proteolysis without receptor-triggered dimerization during drug-induced apoptosis. *J Biol Chem* **2005**, 280(7), 5267–5273.

61. Estornes. Y.; Aguileta, M.A.; Dubuisson, C.; Keyser, J. D.; Goossens, V.; Kersse, K.; Samali, A.; Vandenabeele, P.; Bertrand, M.J. M. RIPK1 promotes death receptor-independent caspase-8-mediated apoptosis under unresolved ER stress conditions. *Cell Death Dis* **2014**, 5, e1555.

62. Zhong, B., Liu, M., Bai, C.; Ruan, Y.; Wang, Y.; Qiu, L.; Hong, Y.; Wang, X.; Li, L.; Li, B. Caspase-8 induces lysosome-associated cell death in cancer cells. *Mol Ther* **2020**, 28(4), 1078-1091.

63. Pan, J.; Xu, G.; Yeung, S. J. Cytochrome *c* release is upstream to activation of caspase-9, caspase-8, and caspase-3 in the enhanced apoptosis of anaplastic thyroid cancer cells induced by Manumycin and Paclitaxel. *J Clin Endocrinol Metab* **2001**, 86(10), 4731–4740.

64. Viswanath, V., Wu, Y., Boonplueang, R., Chen, S., Stevenson, F. F.; Yantiri, F., Yang, L.; Beal, M. F.; Andersen, J. K. Caspase-9 activation results in downstream caspase-8 activation and bid cleavage in 1-methyl-4-phenyl-1,2,3,6-tetrahydropyridine induced Parkinson's disease. *J Neurosci* **2001**, 21(24), 9519–9528.

65. Li, P.; Zhou, L.; Zhao, T.; Liu, X.; Zhang, P.; Liu, Y.; Zheng, X.; Li, Q. Caspase-9: structure, mechanisms and clinical application. *Oncotarget* **2017**, 8(14), 23996-24008.

66. Avrutsky, M. I.; and Troy, C. M. Caspase-9: A multimodal therapeutic target with diverse cellular expression in human disease. *Front Pharmacol* **2021**, 12, 701301.

Porter, A. G.; Janicke, R. U. Emerging roles of caspase-3 in apoptosis. *Cell Death Differ* **1999**, 6, 99–104.

67. Li, J.; Yuan, J. Caspases in apoptosis and beyond. *Oncogene* **2008**, 27, 6194–6206.

68. Engels, I. H.; Stepczynska, A.; Stroh, C.; Lauber, K.; Berg, C.; Schwenzer, R., Wajant, H.; Janicke, R. U.; Porter, A. G.; Belka, C.; Gregor, M.; Schulze-Ostho, K.; Wesselborg, S. Caspase-8/FLICE functions as an executioner caspase in anticancer drug-induced apoptosis. *Oncogene* **2000**, 19, 4563–4573.

69. Brentnall, M., Rodriguez-Menocal, L., De Guevara, R. L.; Cepero, E.; Boise, L. H. Caspase-9, caspase-3 and caspase-7 have distinct roles during intrinsic apoptosis. *BMC Cell Biol* **2013**, 14, 32.

70. Yadav, P.; Yadav, R.; Jain, S.; Vaidya, A. Caspase-3: A primary target for natural and synthetic compounds for cancer therapy. *Chem Biol Drug Des* **2021**, 1–22.

71. Elmore, S. Apoptosis: A review of programmed cell death. *Toxicol Pathol* **2007**, 35(4), 495–516.

72. Rieger, A.M.; Nelson, K. L.; Konowalchuk, J. D.;, Barreda, D. R. Modified annexin V/propidium iodide apoptosis assay for accurate assessment of cell death. *J Vis Exp* **2011**, 50, e2597.

73. Raffray, M.; Cohen, G. M. Apoptosis and necrosis in toxicology: A continuum or distinct modes of cell death? *Pharmacol Ther* **1997**, 75(I), 153-177.

74. Escobar, M. L.; Echeverría, O. M.; Vázquez-Nin, G. H. Necrosis as programmed cell death. In *Cell death - Autophagy, Apoptosis and Necrosis*. Ntuli, T. M.; Ed.; IntechOpen, 2015; pp. 420-434.

75. Kotala, V.; Uldrijan, S.; Horky, M.; Trbusek, M.; Strnad, M; Vojtesek, B. Potent induction of wild-type p53-dependent transcription in tumour cells by a synthetic inhibitor of cyclin-dependent kinases. *Cell Mol Life Sci* **2001**, 58, 1333–9.

76. Wen, J., You, K.; Lee, S.; Song, C.; Kim, D. Oxidative stress-mediated apoptosis. *J Biol Chem* **2002**, 277(41), 38954–38964.

77. Shang, H.; Chang, C.; Chou, Y.; Yeh, M.; Au, M.; Lu, H.; Chu, Y.; Chou, H.; Chou, H.; Shih, Y.; Chung, J. Curcumin causes dna damage and affects associated protein expression in Hela human cervical cancer cells. *Oncol Rep* **2016**, 36, 2207-2215.

78. González-Burgos, E.; Gómez-Serranillos, M.P. Terpene compounds in nature: A review of their potential antioxidant activity. *Curr Med Chem* **2012**, 19*,* 5319-5341.

79. Hadem, K.L. H.; Sen, A. Identifcation of compounds of *Aristolochia tagala* and apoptotic activity in HeLa cells. *Phcog Mag* **2018**, 14, S571-7.

80. Hadem, K. L. H.; Sen, A. *In vitro* free radical scavenging activity of *Aristolochia tagala.* *Int J Curr Pharm Res* **2018**, 10(4), 40-42.

81. Morla S, Kumar A, Kumar S. Newcastle disease virus mediated apoptosis and migration inhibition of human oral cancer cells: A probable role of β-catenin and matrix metalloproteinase-7. Sci Rep. 2019 Jul 26;9(1):10882.

FIGURE LEGEND:

Figure 1. IC_{50} (µg/mL) of *C. angustifolia* (CAu), *C. amada* (CAm) and *C. caesia* (CCa) required to scavenge 50 % of free radicals DPPH, $ABTS^{\bullet+}$, nitric oxide radical ($NO^{\bullet}$), superoxide radical ($O_2^{\bullet-}$).

Figure 2. Percentage inhibition of proliferation of HeLa cells (A) and SAS cells (B) after treatment with *C. angustifolia* (CAu), *C. amada* (CAm) and *C. caesia* (CCa) for 48 h.

Figure 3: Fluorescence microscopic study of the morphological evaluation of HeLa (A) and SAS (B) cells stained with Hoechst after treatment *C. angustifolia* (CAu), *C. amada* (CAm) and *C. caesia* (CCa) for 48 h compared to untreated control, bar = 5 µm.

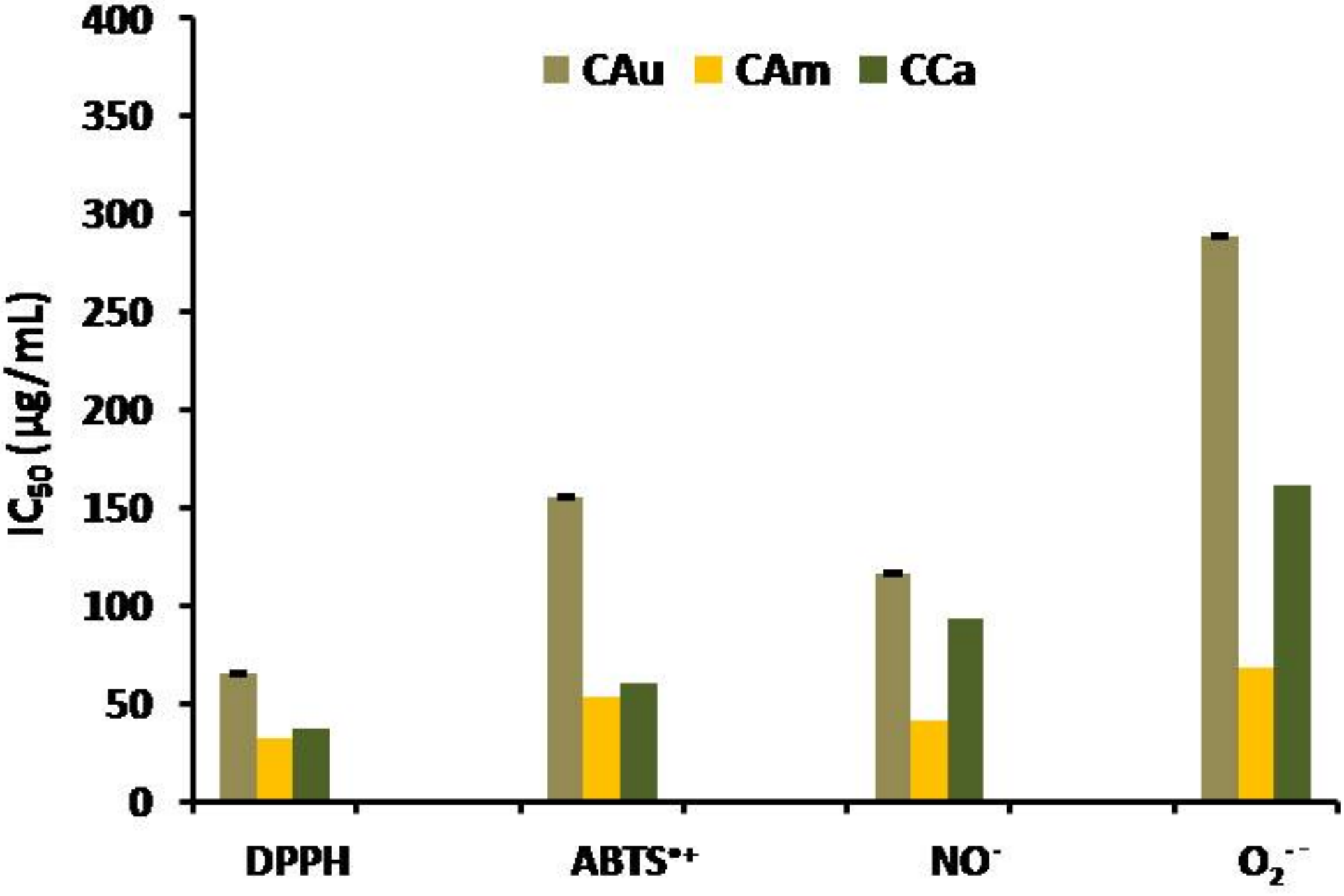
Figure 4: Fuorescence activated cell sorting of HeLa cells (A) and SAS cells (B) treated with *C. angustifolia* (CAu), *C. amada* (CAm) and *C. caesia* (CCa). Annexin-V positive cells (early apoptotic cells, lower right quadrant) and Annexin V/Propidium Iodide double positive (late apoptotic cells, upper right quadrant) and Propodium Iodide positive (necrotic cells, upper left quadrant).

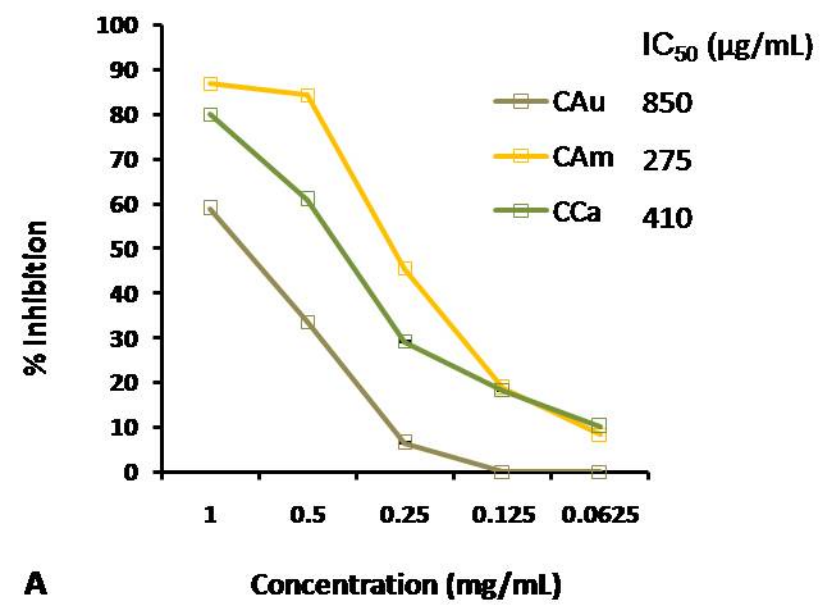
Figure 5: Western blotting analysis of protein immunoblotted with antibodies against p53, Cdk1 and GAPDH. (A) HeLa cells (B) SAS cells post treatment with *C. angustifolia* (CAu), *C. amada* (CAm) and *C. caesia* (CCa) for 24 h. % intensity of p53 and Cdk1 bands were analysed using ImageJ Software and data (relative density normalized to GAPDH) were plotted.

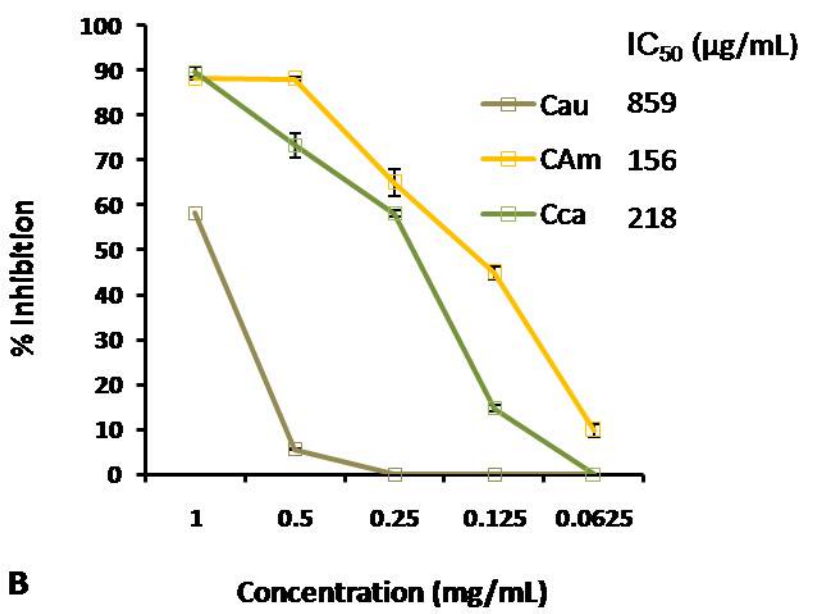
Figure 6: Digital image of HeLa (IA) and SAS (IB) immunoprobe with caspase-8, without treatment (Control) and treatment with *C. angustifolia* (CAu), *C. amada* (CAm) and *C. caesia* (CCa) for 24 h. Nuclei were stained with Hoechst (blue). Some of the cells undergoing apoptosis are indicated with yellow arrows. Bar graph showing fluorescence intensity of treated HeLa cells (IA) and SAS cells (IB) in comparison to their respected untreated controls, bar = 10 µm.

Figure 7: Digital image of HeLa (IIA) and SAS (IIB) immunoprobe with caspase-9, without treatment (Control) and treatment with *C. angustifolia* (CAu), *C. amada* (CAm) and *C. caesia* (CCa) for after 24 h. Nuclei were stained with Hoechst (blue). Some of the cells undergoing apoptosis are indicated with yellow arrows. Bar graph showing fluorescence intensity of treated HeLa cells (IIA) and SAS cells (IIB) in comparison to their respected untreated controls, bar = 10 µm.

Figure 8: Digital image of HeLa (IIIA) and SAS (IIIB) immunoprobe with caspase-3 without treatment (Control) and treatment with *C. angustifolia* (CAu), *C. amada* (CAm) and *C. caesia* (CCa) for after 24 h. Nuclei were stained with Hoechst (blue). Some of the cells undergoing apoptosis are indicated with yellow arrows. Bar graph showing fluorescence intensity of treated HeLa cells (IIIA) and SAS cells (IIIB) in comparison to their respected untreated controls, bar = 10 µm.


400
350
300
250
200
150
100
50
0
IC50 (µg/mL)
CAu
CAm
CCa
DPPH
ABTS•+
NO-
O2•-


100
90
80
70
60
50
40
30
20
10
0
% Inhibition
IC50 (µg/mL)
CAu 850
CAm 275
CCa 410
1
0.5
0.25
0.125
0.0625
A
Concentration (mg/mL)


100
90
80
70
60
50
40
30
20
10
0
% Inhibition
IC50 (µg/mL)
Cau 859
CAm 156
Cca 218
1
0.5
0.25
0.125
0.0625
B
Concentration (mg/mL)

Control

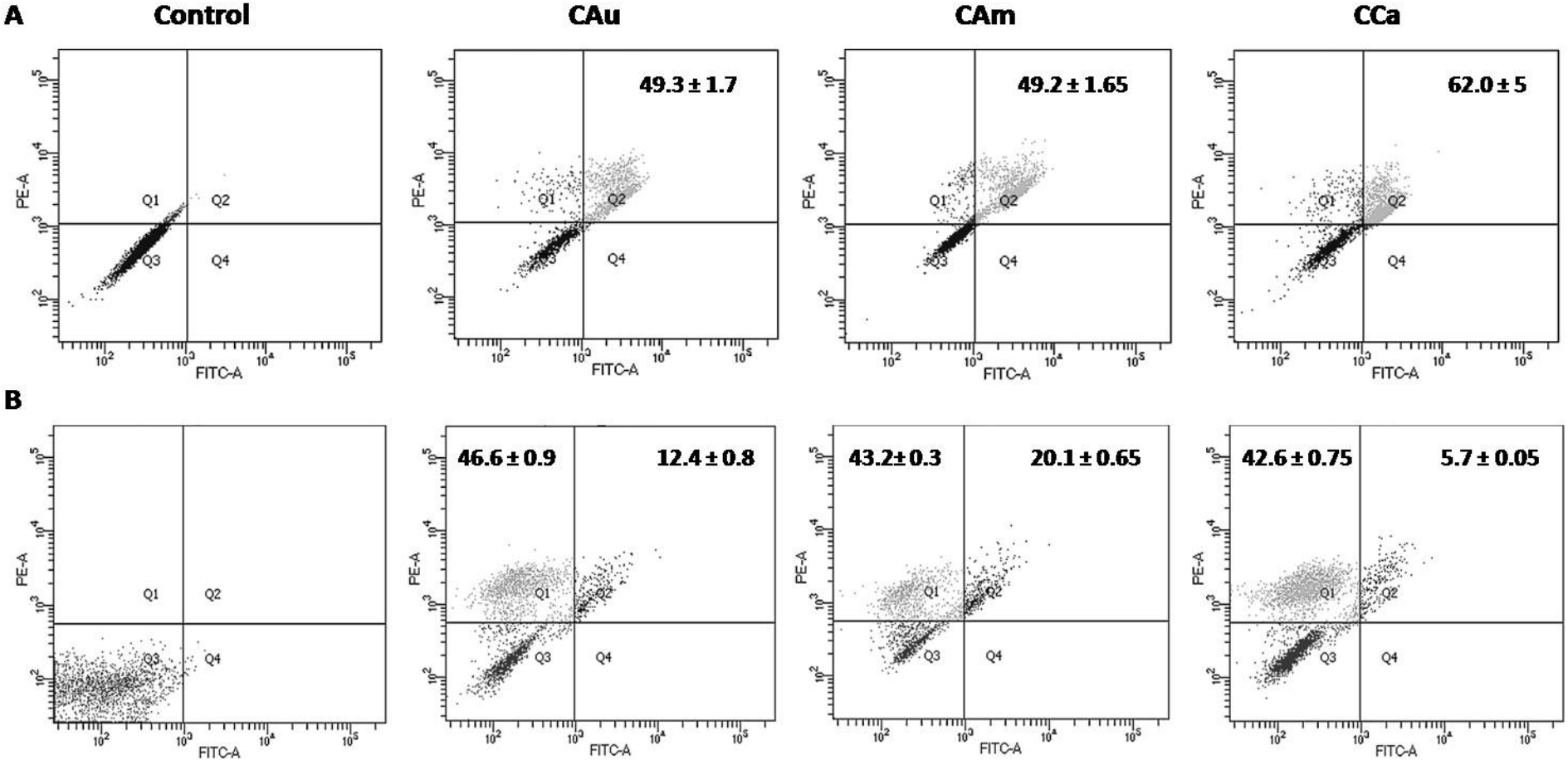
CAu

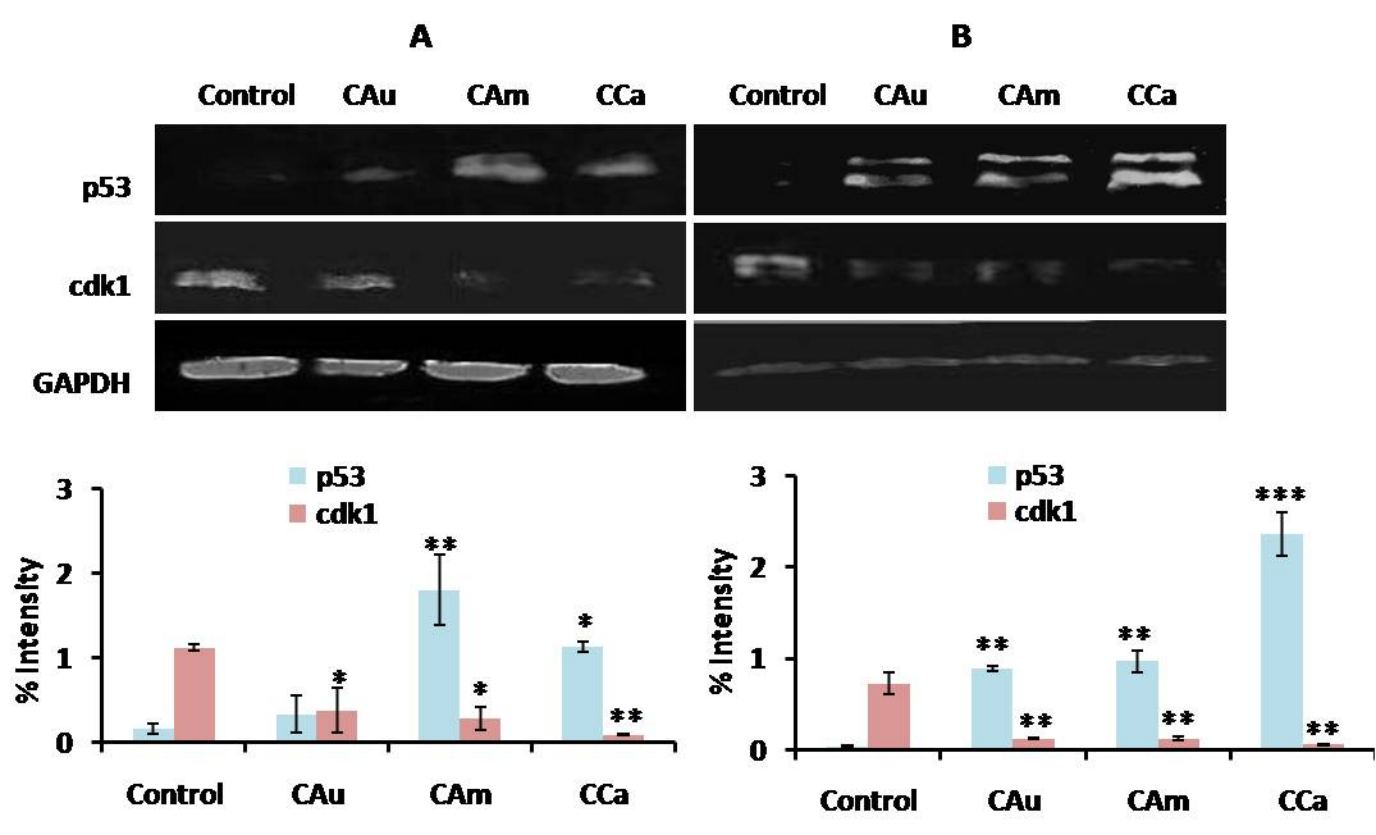
CAm

CCa

A

B


A
Control
CAu
CAm
CCa
49.3 ± 1.7
49.2 ± 1.65
62.0 ± 5
B
46.6 ± 0.9
12.4 ± 0.8
43.2± 0.3
20.1 ± 0.65
42.6 ± 0.75
5.7 ± 0.05
PE-A
FITC-A
Q1
Q2
Q3
Q4


A
B
Control
CAu
CAm
CCa
Control
CAu
CAm
CCa
p53
cdk1
GAPDH
p53
cdk1
% Intensity
3
2
1
0
Control
CAu
CAm
CCa
p53
cdk1
% Intensity
3
2
1
0
Control
CAu
CAm
CCa

GFP

Hoechst

Merge

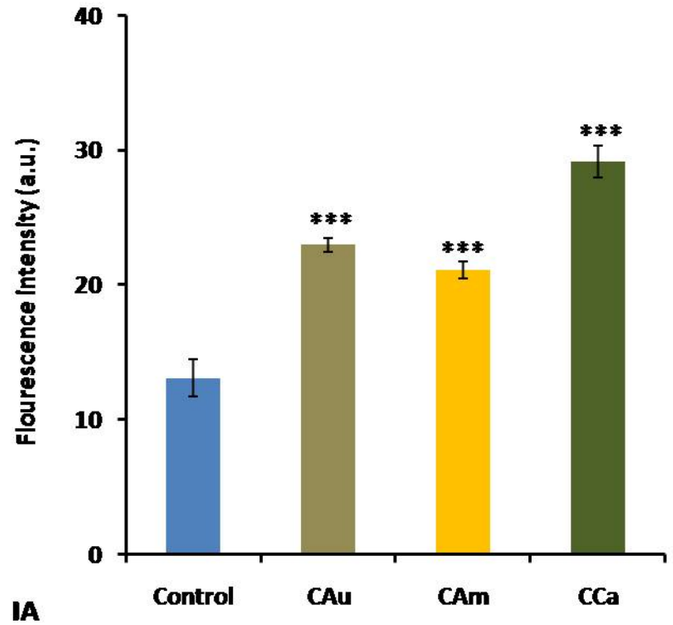
IA

Control

CAu

CAm

CCa



IA

GFP

Hoechst

Merge

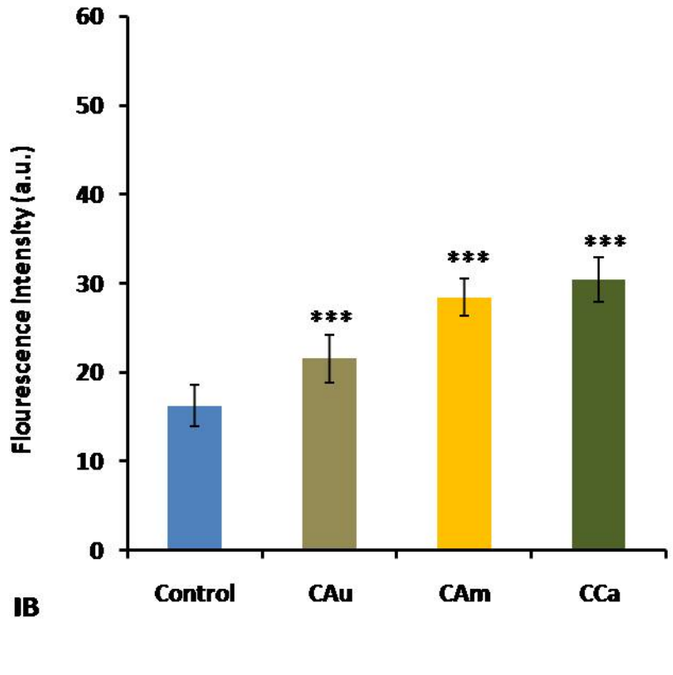
IB

Control

CAu

CAm

CCa



IB

GFP

Hoechst

Merge

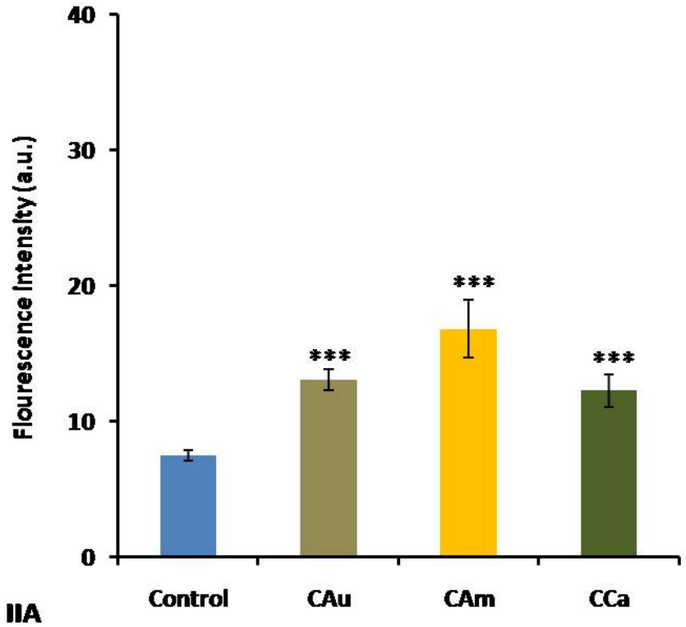
IIA

Control

CAu

CAm

CCa



IIA

GFP

Hoechst

Merge

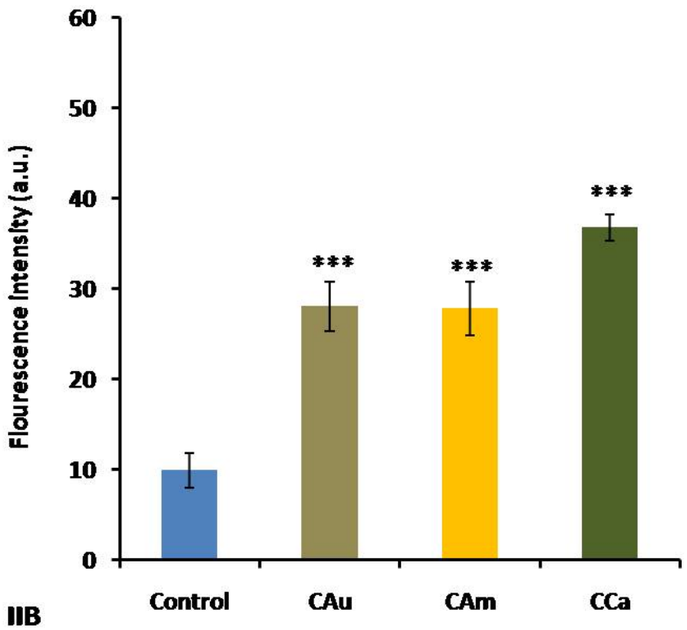
IIB

Control

CAu

CAm

CCa



IIB

GFP

Hoechst

Merge

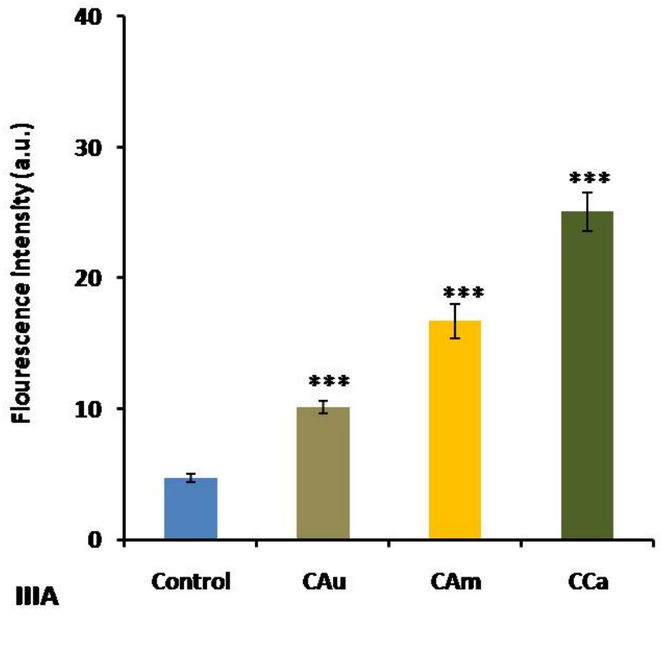
IIIA

Control

CAu

CAm

CCa



GFP

Hoechst

Merge

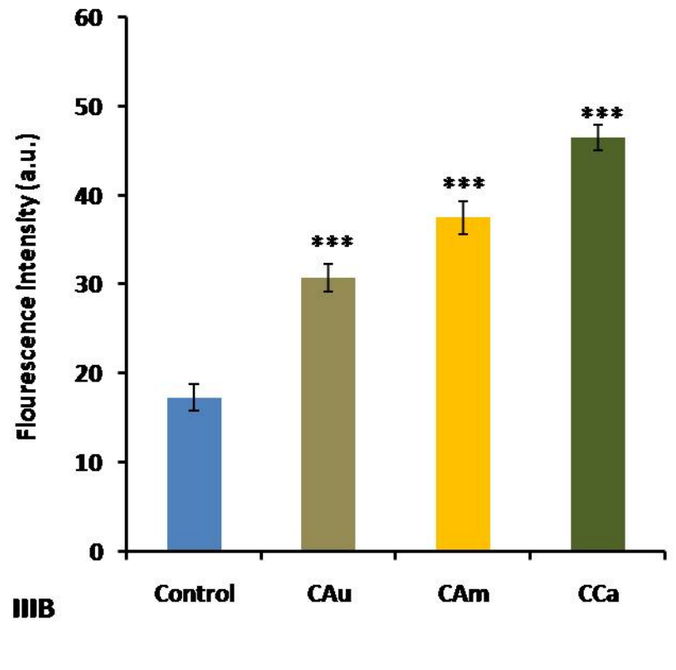
IIIB

Control

CAu

CAm

CCa



IIIB

Supplementary Files

This is a list of supplementary files associated with this preprint. Click to download.

- FulluncroppedGelsBlotsalongwithlegendsforSupplementary231026.docx